

A test-particle model of the atmosphere/ionosphere system of Saturn's main rings

M. Bouhram,¹ R. E. Johnson,² J.-J. Berthelier,¹ J.-M. Illiano,¹ R. L. Tokar,³ D. T. Young,⁴ and F. J. Crary⁴

Received 20 October 2005; revised 12 January 2006; accepted 24 January 2006; published 15 March 2006.

[1] The first pass of the Cassini orbiter near the A and B rings of Saturn, formed mainly by H₂O ice particles, revealed the presence of an ionosphere composed of O⁺ and O₂⁺ ions. Such a result suggests the existence of an atmospheric halo made up of molecular oxygen surrounding the rings. It is produced by solar UV radiation-induced decomposition of ice releasing molecular oxygen which does not stick on the surface at the relevant temperatures. A Monte Carlo model of the atmosphere/ionosphere ring system that uses test-particles and incorporates chemical processes and transport of both neutrals and plasma ions is developed. Published ion data from the ion mass spectrometer (IMS) experiment were used as constraint and the model provides a very satisfactory fit between simulated O⁺ and O₂⁺ ion densities and those measured along Cassini trajectory. **Citation:** Bouhram, M., R. E. Johnson, J.-J. Berthelier, J.-M. Illiano, R. L. Tokar, D. T. Young, and F. J. Crary (2006), A test-particle model of the atmosphere/ionosphere system of Saturn's main rings, *Geophys. Res. Lett.*, 33, L05106, doi:10.1029/2005GL025011.

1. Introduction

[2] A tenuous atmosphere surrounding Saturn's main rings was predicted to exist as a consequence of sputtering of atoms and molecules from ring particles due to collisions by energetic ions and meteoroid particles [Pospieszalska and Johnson, 1991; Ip, 1984a, 1995] or solar photons [Carlson, 1980]. However, until the arrival of the Cassini mission in the vicinity of Saturn, the region near the inner A and B rings remained unexplored and models were based on numerous assumptions that could not be directly tested.

[3] Plasma measurements in Saturn's magnetosphere during Cassini's orbit insertion, particularly those from the Cassini Plasma Spectrometer (CAPS) experiment [Young *et al.*, 2004] and the Ion Neutral Mass Spectrometer [Waite *et al.*, 2004], provided a remarkably consistent picture of the plasma environment. An initial analysis of the data revealed the presence of an ionosphere close to the A and B rings with O⁺ and O₂⁺ as major ions, suggesting the existence of an atmosphere made up of molecular oxygen O₂ [Young *et al.*, 2005; Tokar *et al.*, 2005; Waite *et al.*, 2005]. This O₂

atmosphere is likely to be a significant source of plasma for Saturn's magnetosphere, in addition to the E-ring, icy satellites and Titan, since Tokar *et al.* [2005] also showed that O₂⁺ extends into the magnetosphere inside the F and G rings and energetic O₂⁺ ions were observed throughout the magnetosphere [Krimigis *et al.*, 2005]. Because the Cassini orbiter will not fly close to the A and B rings again, a detailed description of the O₂ atmosphere is now required to quantify its role as plasma source for Saturn's magnetosphere.

[4] In this paper, we present preliminary results of a study based on a 2D hybrid model of the ring atmosphere/ionosphere system. The model uses a test particle approach for both ions and neutrals similar to that used by J. G. Luhmann *et al.* (A model of the ionosphere of Saturn's rings and its implications, submitted to *Icarus*, 2006, hereinafter referred to as Luhmann *et al.*, submitted manuscript, 2006). It takes into account chemical processes, such as photoionization and charge exchange, by means of Monte Carlo particle tracking to describe the transport. The simulation results are then compared with published ion data from the ion mass spectrometer (IMS) experiment and rough overall agreement is found.

2. Geometry and Model

[5] Figure 1 shows the Cassini trajectory during Saturn's orbit insertion (SOI) maneuver. O₂ is produced on the sunlit side, with the sun 23.6° south of the ring plane, by UV photons while the flyby occurred north of the ring plane. This trajectory provided the first in-situ measurements over Saturn's A and B rings.

2.1. A model of the O₂ Atmosphere

[6] The rings consist mainly of H₂O ice particles from which O₂ molecules are primarily produced by solar UV photons. Although O₂ is produced inefficiently from ice, compared to water molecules and water fragments, at the surface temperature of the icy grains (80–100°K), O₂ molecules do not stick on the ice particles while other products and ions do [Young *et al.*, 2005; Johnson *et al.*, 2006]. This explains why O₂ is the main constituent of the ring atmosphere, as is also the case for Jupiter's icy satellite Europa [Shematovich *et al.*, 2005].

[7] In this model, the production and formation of ring neutral atmosphere is described following the model proposed by Johnson *et al.* [2006]. O₂ molecules, originating from the radiation-induced decomposition of ice, are produced primarily by UV photons which are absorbed on the south side of the ring plane at a rate $(1 - f)S_{O_2}$. Here S_{O_2} is estimated to be $10^6 \text{ cm}^{-2} \text{ s}^{-1}$ [Westley *et al.*, 1995; Johnson *et al.*, 2006] and $f = \exp(-\xi/\cos \gamma)$ is determined by the

¹Centre d'Étude des Environnements Terrestre et Planétaires, Saint-Maur, France.

²Material Science and Engineering, University of Virginia, Charlottesville, Virginia, USA.

³Los Alamos National Laboratory, Los Alamos, New Mexico, USA.

⁴Southwest Research Institute, San Antonio, Texas, USA.

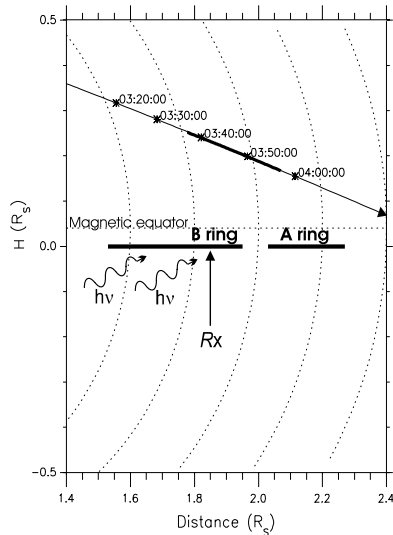


Figure 1. Drawing that shows the simulation domain and the trajectory of the Cassini orbiter during Saturn's orbit insertion (SOI) on July 1, 2004. The dipole field lines are indicated. The vertical axis gives z and the horizontal axis gives the radial distance along the magnetic equator.

optical thickness of the ring ξ and $\gamma = 66^\circ$ the incidence of UV photons with respect to the ring plane's normal. According to stellar occultation measurements on Voyager 2 [Esposito *et al.*, 1983], we set $\xi = 0.01$ for $r < 1.53 R_S$, $\xi = 1.0$ in the B ring ($1.53 R_S < r < 1.95 R_S$), $\xi = 0.06$ in the Cassini gap ($1.95 R_S < r < 2.03 R_S$), $\xi = 0.50$ in the A ring ($2.03 R_S < r < 2.26 R_S$), and $\xi = 10^{-5}$ for $r > 2.26 R_S$. Particles are ejected south of the ring plane at random positions, but with appropriate account for the radial variation of ξ . They are ejected at a speed equal to the Keplerian velocity V_o plus a component in a random direction following a non-thermal energy distribution inferred from experimental measurements in laboratory [Johnson *et al.*, 1983]: $F(E) \propto U/(E + U)^2$ where $U = 0.015 \text{ eV}$. This later velocity component is small compared to V_o .

[8] In one bounce period, O_2 molecules return to the ring plane and are absorbed onto a ring particle with a probability of $P = 1 - \exp(-\xi/\cos \alpha)$ where α is the incident angle between the velocity in the ring frame and the normal to the ring plane and ξ is defined above. This probability is relatively high (>0.5) inside the A and B rings, because of their low transparencies ($\xi > 0.5$), but small outside of those regions. Because O_2 does not stick on the ice at the relevant temperatures (80–100°K), we assume that when such a particle hits the rings, it is directly re-emitted without any energy loss. Earlier, we assumed it was thermalized before re-emission [Johnson *et al.*, 2006], but this difference has a negligible effect on the simulation results. In contrast, O , O_2^+ and O^+ particles stick/react and, therefore, are absorbed or react when hitting a ring particle.

2.2. Ion Production and Transport

[9] O_2^+ and O^+ ions are created in the ring plane environment by means of Monte Carlo techniques from photo-

ionization and photodissociation of O_2 , with average frequencies $k_i = 9.1 \times 10^{-9} \text{ s}^{-1}$ and $k_d = 2.5 \times 10^{-9} \text{ s}^{-1}$, respectively. This favors O_2^+ by a branching ratio $k_i/k_d \sim 3.6$. Note also that O^+ is created with the O_2 speed plus a significant excess energy ($\sim 0.5 \text{ eV}$) in a random direction [Luna *et al.*, 2005], while a newly formed O_2^+ ion receives no excess energy. In addition, we consider the charge exchange reaction $O_2 + O_2^+ \rightarrow O_2^+ + O_2$. Although this reaction does not modify the O_2^+ density, it is important for redistributing ion velocities and, therefore, populating ion pitch angles. This depends on the relative speed V_{rel} between O_2 and O_2^+ . When V_{rel} is small, the new velocity is equal to the center-of-mass velocity plus a velocity in a random direction that is equal to half of the relative collision speed and use the cross section of Johnson *et al.* [2006]. In contrast, when V_{rel} is large, ion and neutral velocities are exchanged. In this model, we set the transition limit between the two regimes at $V_{rel} \sim 10 \text{ km s}^{-1}$. Because V_{rel} is on average small in the region where CAPS data are available, between 1.8 and 2.1 R_S , simulation results are not sensitive to this parameter.

[10] Ions created in the vicinity of the ring plane are picked up by the magnetic field of Saturn B and the corotating electric field $E = V_{co} \times B$ where $V_{co} = \Omega_S \times r$ is the corotation velocity. Assuming that neutrals have a speed close to the Keplerian speed V_o plus a small thermal component V_{th} acquired during the surface ejection process, newly formed ions gyrate about the magnetic field at a speed $\sim V_o - V_{co}$, and move around the planet at V_{co} . In the absence of collisions with ring particles, ions move up the field lines and are reflected by the magnetic mirror force formed by converging field lines at a magnetic latitude that depends on their initial pitch angle. Because $V_o - V_{co}$ is approximately perpendicular to the magnetic field, ions are created with a pitch angle $\sim 90^\circ$, leading to high incident angles $\alpha \sim 90^\circ$ when returning to the ring plane. This is the case except near $R_X = 1.86 R_S$ where $V_o = V_{co}$ and consequently the term V_{th} dominates the gyration velocity (see Figure 1), enabling ions to reach higher latitudes, and leading to higher transmission probabilities across the ring plane near R_X .

[11] The particle motion is traced by solving the guiding center motion's equation [Northrop, 1963], taking into account the effect of gravity, magnetic field and corotating electric fields. For a planetocentric distance smaller than 8 R_S , we may approximate the magnetic field of Saturn as a dipole with an offset with respect to the ring plane by 0.04 R_S toward the North along the rotation axis (see Figure 1).

[12] A neutral source is generated starting with 2×10^4 O_2 test particles injected between 1.4 and 2.4 R_S that are followed versus time until they are lost through Saturn's surface or by creating O_2^+ and O^+ ions. Both ion and neutral trajectories are calculated using a Runge-Kutta fourth-order integration scheme with a fixed time step Δt . The ions are tracked until they are lost through the rings or Saturn's surface. In our simulations, the number density and higher-order particle moments are obtained by scaling the total number of test-particle ions employed to the photo-production rate, similar to method used by Ip [1995]. The system is divided into grid points assuming a cylindrical symmetry with a uniform step $\Delta \rho = 0.02 R_S$ in radial position, and a non-uniform step in height from $\Delta z = 2 \times$

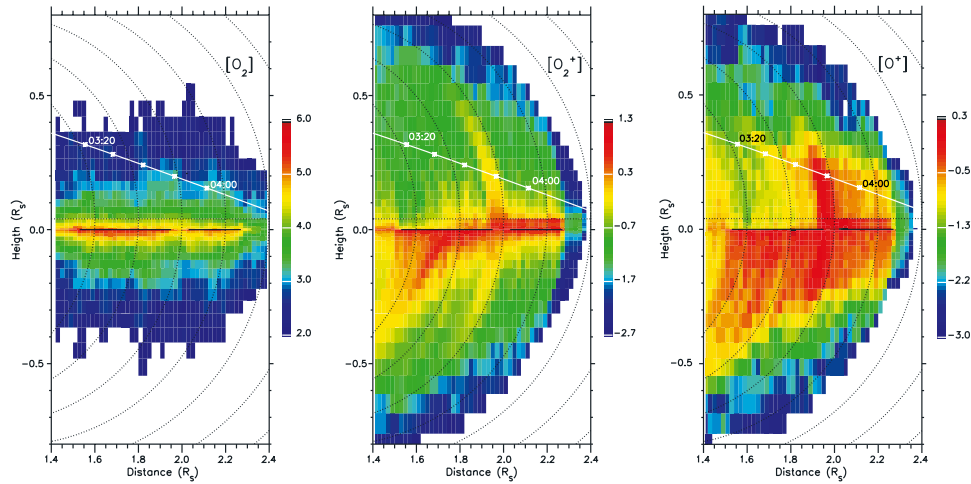


Figure 2. From left to right, particle density maps in $\text{Log}(\text{cm}^{-3})$ of O_2 , O_2^+ and O^+ . The axes are the same as in Figure 1.

$10^{-3} R_S$ near the ring plane to $0.02 R_S$ at the top. At time step $t_n = n\Delta t$, the position of the test-particle is binned into appropriate cell element (ρ, z) in which it is located.

3. Results and Discussion

[13] Figure 2 shows two-dimensional maps of O_2 , O_2^+ and O^+ number densities inferred from test-particles trajectories. First, we see that due to its long lifetime $\tau = 1/(k_i + k_d) \sim 8.6 \times 10^7 \text{s}$, O_2 exists both above and below the ring plane. Assuming that O_2 behaves as a gas in equilibrium, we may express the atmospheric scale height as $h_{\text{O}_2} = (2k_B T_n / 3m_n \Omega_S^2)^{1/2} \sim 1.3 \times 10^{-2} R_S$, which is consistent with our simulations (not shown) and our earlier analytic model [Johnson *et al.*, 2006]. Luhmann *et al.*, submitted manuscript (2006) showed, using a test-particle approach, that the average ion scale height grew with increasing ρ beyond $R_X = 1.86 R_S$ but inside of that radius the ion trajectories decayed with the ions precipitating into Saturn's ionosphere. As suggested Connerney and Waite [1984], the presence of an influx from the B-ring may explain the diurnal variations of maximum ionospheric electron density deduced from earlier measurements. Here we find similar results but also include the impact/transmission probability for ions to pass through the rings. Indeed, it is shown in addition that the O_2^+ and O^+ density distributions exhibit a strong asymmetry between the sunlit and shaded sides of the B ring, because of its low transparency ($\xi = 1.0$). In contrast, ions may easily bounce inside the Cassini gap where the transparency is very high ($\xi = 0.06$).

[14] Figure 3 provides comparisons between simulated O_2^+ , O^+ and total ion number densities with those measured by the IMS experiment along the orbiter's trajectory and published by Tokar *et al.* [2005]. At distances $\rho < 1.92 R_S$, Cassini is on magnetic field lines that map to the B-ring where ion production is small so that local ion densities are primarily controlled by the ion transmission probabilities through the ring plane. As discussed earlier, this probability increases when the ring optical depth ξ and the ion incident angle α both decrease. For O_2^+ ions, two bumps in the density are observed and are nicely reproduced by the model. The first one at $\rho \sim 1.79 R_S$ corresponds to the field lines that map at $L \sim R_X$ where $V_o = V_{co}$ and O_2^+ incident

angles are more isotropic than anywhere else. At the boundary between the B-ring and the Cassini gap, the change in ξ and ion production rates on the northern side leads to a second density increase. Only the second feature is found for O^+ because these ions are produced with an excess energy ($\sim 0.5 \text{ eV}$) higher than their corotation energy in the ring frame ($< 0.3 \text{ eV}$), and therefore achieve nearly isotropic incident angles over the B-ring. As Cassini passes above the A-ring after $\rho \sim 2.07 R_S$, CAPS was not facing the corotation direction anymore, but the INMS experiment reported some ion measurements that indicates the presence of O_2^+ , O^+ and H^+ ions, contributing to about 43%, 13% and 44% of the total density, respectively [Waite *et al.*, 2005]. Here, our simulation results indicate a density ratio $[\text{O}_2^+]/[\text{O}^+] \sim 3$, consistent with INMS data. We have also compared the total simulated ion density $N_i = [\text{O}_2^+] + [\text{O}^+]$ with the one from IMS. Here, the vertical bars were inferred from comparisons with other measurements of charge density [see Tokar *et al.*, 2005, Figure 4]. Tokar *et al.* [2005] showed that IMS total densities are underestimated above the Cassini division and attributed these differences to uncertainties in the precise relative IMS detector efficiencies, but one cannot completely exclude the possible presence of H^+ ions that have too low energies for being detected. The fact that light ions are not included in the model may explain why the simulated total density is

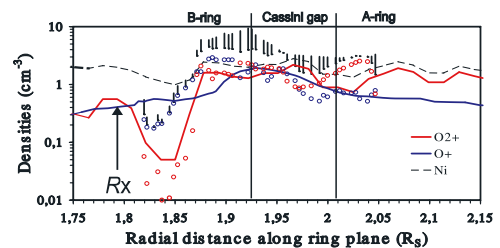


Figure 3. Measured (open circles) and simulated (solid curves) O_2^+ (blue), and O^+ (red) ion densities along Cassini trajectory in cm^{-3} . Vertical bars indicate measurements of the total ion density while the dashed curve shows the simulated total ion density. The vertical lines indicate the boundaries of the Cassini gap.

underestimated as well. In contrast, simulated densities are overestimated above the B-ring for O_2^+ and partly for O^+ . A mechanism that has been ignored but may potential play a role is the electrostatic charge state of the grains. This charging depends in part on the UV photoelectron emission from its sunlit surface, but also on the electron and ion fluxes in the ambient plasma surrounding the grain [Ip, 1984b]. Charging will modify the interaction between the grains and the plasma particles. If grains are negatively charged, as suggested by electron measurements above the rings [Coates *et al.*, 2005], the probability of collision with ions (electrons) would increase (decrease). We also neglected in the present model the ambipolar electric field due to the charge separation between electrons and ions near the ring plane [Wilson and Waite, 1989; Moncuquet *et al.*, 2002]. In the regions associated with a strong density gradient, this additional electric field along the magnetic field lines may modify the electron and ion scale heights, as discussed by Johnson *et al.* [2006]. These effects can be taken into account only in a self consistent manner by incorporating the electron dynamics, which is beyond the scope of the present paper. A more elaborate model is needed for further improvement in the regions associated with strong inhomogeneities, and will be subject of a future paper.

[15] **Acknowledgments.** The work at CETP on the CAPS experiment is supported by the Centre National d'Etudes Spatiales under contract CNES EU282. M.B. is grateful to CNES for its financial support. We thank the entire CAPS team, JPL Cassini project and all the funding agencies which made CAPS a success. Work in the United States was performed under JPL contract 1243218 with Southwest Research Institute.

References

- Carlson, R. W. (1980), Photosputtering of Saturn's rings, *Nature*, *283*, 461–463.
- Coates, A. J., *et al.* (2005), Plasma electrons above Saturn's main rings: CAPS observations, *Geophys. Res. Lett.*, *32*, L14S09, doi:10.1029/2005GL022694.
- Connery, J. E. P., and J. H. Waite (1984), New model of Saturn's ionosphere with an influx of water from the rings, *Nature*, *312*, 136–138.
- Esposito, L. W., M. Ocallaghan, K. E. Simmons, C. W. Hord, R. A. West, A. L. Lane, R. B. Pomphrey, D. L. Coffeen, and M. Sato (1983), Voyager photopolarimeter stellar occultation of Saturn's rings, *J. Geophys. Res.*, *88*, 8643–8649.
- Ip, W.-H. (1984a), Plasmatization and recondensation of the Saturnian rings, *Nature*, *320*, 143–145.
- Ip, W.-H. (1984b), Electrostatic charging of the rings of Saturn: A parameter study, *J. Geophys. Res.*, *89*, 3829–3836.
- Ip, W.-H. (1995), Exospheric systems of Saturn's rings, *Icarus*, *115*, 295–303.
- Johnson, R. E., J. W. Boring, C. T. Reimann, L. A. Barton, J. W. Sieveka, J. W. Garrett, K. P. Farmer, W. L. Brown, and L. J. Lanzerotti (1983), Plasma ion-induced molecular ejection on the Galilean satellites: Energies of the ejected molecules, *Geophys. Res. Lett.*, *10*, 892–895.
- Johnson, R. E., J. G. Luhmann, R. L. Tokar, M. Bouhram, J. J. Berthelier, E. C. Sittler, J. F. Cooper, T. W. Hill, F. J. Cray, and D. T. Young (2006), Production, ionization and redistribution of Saturn's O_2 ring atmosphere, *Icarus*, *180*, 393–402.
- Krimigis, S. M., *et al.* (2005), Dynamics of Saturn's magnetosphere from MIMI during Cassini's orbital insertion, *Science*, *307*, 1270–1273.
- Luna, L. C., C. McGrath, M. B. Shah, R. E. Johnson, C. J. Latimer, and E. C. Montenegro (2005), Dissociative charge exchange and ionization of O_2 by fast H^+ and O^+ ions: Energetic ion interactions in the Europa's oxygen atmosphere and neutral torus, *Astrophys. J.*, *628*, 1086–1096.
- Moncuquet, M., F. Bagenal, and N. Meyer-Vernet (2002), Latitudinal structure of outer Io plasma torus, *J. Geophys. Res.*, *107*(A9), 1260, doi:10.1029/2001JA900124.
- Northrop, T. G. (1963), *The Adiabatic Motion of Charged Particles*, John Wiley, New York.
- Pospieszalska, M. K., and R. E. Johnson (1991), Micrometeorite erosion of the main rings as a source of plasma in the inner Saturnian plasma torus, *Icarus*, *93*, 45–52.
- Shematovich, V. I., R. E. Johnson, J. F. Cooper, and M. C. Wong (2005), Surface-bounded atmosphere of Europa, *Icarus*, *173*, 480–498.
- Tokar, R. L., *et al.* (2005), Cassini observations of the thermal plasma in the vicinity of Saturn's main rings and the F and G rings, *Geophys. Res. Lett.*, *32*, L14S04, doi:10.1029/2005GL022690.
- Waite, J. H., *et al.* (2004), The Cassini ion and neutral mass spectrometer (INMS) investigation, *Space Sci. Rev.*, *114*, 113–231.
- Waite, J. H., *et al.* (2005), Oxygen ions observed near Saturn's A ring, *Science*, *307*, 1260–1262.
- Westley, M. S., R. A. Baragiola, R. E. Johnson, and G. A. Baratta (1995), Ultraviolet photodesorption from water ice, *Planet. Space Sci.*, *43*, 1311–1315.
- Wilson, G. R., and J. H. Waite Jr. (1989), Kinetic modeling of the Saturn-ring ionosphere plasma environment, *J. Geophys. Res.*, *94*, 17,287–17,298.
- Young, D. T., *et al.* (2004), Cassini plasma spectrometer investigation, *Space Sci. Rev.*, *114*, 1–112.
- Young, D. T., *et al.* (2005), Composition and dynamics of plasma in Saturn's magnetosphere, *Science*, *307*, 1262–1266.

J.-J. Berthelier, M. Bouhram, and J.-M. Illiano, Centre d'Étude des Environnements Terrestre et Planétaires, F-94100 Saint-Maur, France. (mehdi.bouhram@cetp.ipsl.fr)

R. E. Johnson, Material Science and Engineering, University of Virginia, Charlottesville, VA 22903, USA.

R. L. Tokar, Los Alamos National Laboratory, Los Alamos, NM 87545, USA.

F. J. Cray and D. T. Young, Southwest Research Institute, San Antonio, TX 78228-0510, USA.